Novel manganese(II) and cobalt(II) 3D polymers with mixed cyanate and carboxylate bridges: crystal structure and magnetic properties†‡

Yan-Qin Wang,[a] Kun Wang,[a] Qian Sun,[a] Hua Tian,[a] En-Qing Gao*[a] and You Song[b]

Received 20th July 2009, Accepted 11th September 2009
First published as an Advance Article on the web 30th September 2009
DOI: 10.1039/b914592c

Two isomorphous 3D Mn(II) and Co(II) coordination polymers with a dicarboxylate inner salt and cyanate as coligands were synthesized and structurally characterized, and their magnetic properties have been studied. In the compounds, $[M(L)(NCO)]_n \cdot nH_2O$ (M = Mn, Co, L = 1-carboxymethylpyridinium-4-carboxylate), neighboring metal ions are linked by the 3-fold bridges of an end-on cyanate and two *syn–syn* carboxylate bridges to give an anionic chain of $[M(\mu\text{-}NCO)(\mu\text{–}COO)_2]_n$, and each chain is interlinked to four other chains by the cationic 1-methylpyridinium spacers to generate a 3D structure with the $4^2 \cdot 6^3 \cdot 8$ net topology. They are the first compounds with mixed cyanate and carboxylate bridges. Magnetic studies reveal that the 3-fold mixed bridge propagates antiferromagnetic coupling in the Mn(II) compound but ferromagnetic coupling in the Co(II) compound. The rather complex magnetic behaviors of the Co(II) compound are analyzed taking into account the first-order spin-orbital coupling and the intrachain ferromagnetic interactions.

1 Introduction

The field of molecular magnetic materials has attracted much attention and seen great progress in recent years.[1-2] The materials studied so far consist of extended coordination networks or discrete polynuclear aggregates, in which paramagnetic metal ions are held together by short bridging ligands allowing for sufficiently strong magnetic exchange. The pseudohalide (N_3^-, OCN^-, *etc.*) bridges are among the major players in this field. The azido ion is undoubtedly the most extensively studied pseudohalide bridge for its versatility in bridging metal ions and mediating magnetic coupling.[3-5] Thus, a great number of discrete polynuclear and infinite polymeric metal-azido coordination compounds with a diversity of structural motifs and magnetic properties have been reported.[3-5] By contrast, the cyanate ion is less adequately explored.[3c,6-9] The cyanate anion can bridge metal ions in the end-to-end (EE) or end-on (EO, mostly the N-EO, see Scheme 1) mode. The magnetically studied compounds with cyanate bridges are mainly Cu(II)[8] and Ni(II)[6,9] species, and the magnetic exchange through cyanate is usually weaker than that through azide, the nature depending upon the coordination mode and other structural factors.[6-9] A widely utilized approach to control the magnetic exchange between metal ions is to incorporate a second bridging ligand. The carboxylate group is a good candidate, which itself can efficiently transmit magnetic exchange and has been widely used to construct molecular magnetic materials. In this context, some systems with simultaneous azido and carboxylate bridges have been described, which utilize simple carboxylates (formate or acetate)[10] and pyridyl-derived carboxylate[11-12] as coligand and display a rich diversity of structural and magnetic properties. However, no examples with simultaneous cyanate and carboxylate bridges have been reported to date, despite the similarity of cyanate to azide. Recently, we demonstrated an efficient strategy of constructing mixed azido and carboxylate bridged systems from inner-salt-type dicarboxylate coligands.[13] The use of such ligands, which bear positively charged pyridinium groups, can not only lead to high-dimensional networks, but also help to balance the competition between azide and carboxylate in binding metal ions and compensating the charge of the metal ions. Along this line, here we report the synthesis, structure and magnetic properties of the first metal coordination systems with simultaneous cyanate and carboxylate bridges, $[M(L)(NCO)]_n \cdot nH_2O$ [M = Mn (**1**), Co (**2**); L = 1-carboxymethylpyridinium-4-carboxylate, Scheme 2]. The two compounds are isomorphous and exhibit 3D networks in which anionic chains with uniform cyanate-bis(carboxylate) 3-fold bridges are interlinked by the cationic 1-methylpyridinium spacers. Magnetic studies reveal that the 3-fold mixed bridge propagates antiferromagnetic coupling in **1** but ferromagnetic coupling in **2**. The magneto-structural relationship is discussed qualitatively.

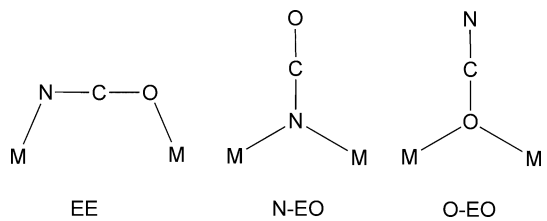

Scheme 1 The bridging modes of cyanate.

[a]*Shanghai Key Laboratory of Green Chemistry and Chemical Processes, Department of Chemistry, East China Normal University, Shanghai, 200062, P.R. China. E-mail: eqgao@chem.ecnu.edu.cn; Fax: 86 21 62233404; Tel: 86 21 62233404*
[b]*State Key Laboratory of Coordination Chemistry, School of Chemistry and Chemical Engineering, Nanjing University, Nanjing, 210093, P.R. China*

† Electronic supplementary information (ESI) available: PXRD graphics. CCDC reference number 739971. For ESI and crystallographic data in CIF or other electronic format see DOI: 10.1039/b914592c

‡ This paper is dedicted to Professor Dai-Zheng Liao on the occasion of his 70th birthday

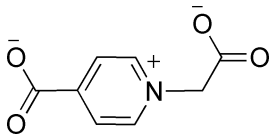

Scheme 2 1-carboxymethylpyridinium-4-carboxylate.

2 Experimental

2.1 General procedure

The reagents were obtained from commercial sources and used without further purification. The ligand L (1-carboxymethylpyridinium-4-carboxylate) was prepared according to the literature.[14]

2.2 Synthesis of 1

A mixture of $Mn(OAc)_2{\cdot}4H_2O$ (0.049 g, 0.2 mmol), L (0.0181 g, 0.1 mmol) and NaOCN (0.026 g, 0.4 mmol) in water/ethanol (3/4 mL) was stirred for 10 min at room temperature. Slow evaporation of the solution at room temperature yielded yellow crystals of **1** after four days. Yield: 60% based on L. Elem. anal. Calcd (%) for $C_9H_8MnN_2O_6$: C, 37.80; H, 2.40; N, 9.80. Found: C, 37.90; H, 2.80; N, 9.90. IR (cm^{-1}, KBr): 2170 s, 1627 s, 1562 m, 1451 m, 1384 s, 1325 m, 758 m, 665 m.

2.3 Synthesis of 2

An ethanol solution (6 ml) of $Co(OAc)_2{\cdot}4H_2O$ (0.10 g, 0.40 mmol) was mixed with the water solution (3 ml) of L (0.072 g, 0.40 mmol), the pink solution was refluxed for 10 minutes, and then NaOCN (0.026 g, 0.4 mmol) was added, yielding a pink polycrystalline precipitate immediately. After refluxing for 4 hours, the solid product was collected by filtration, washed with water and ethanol, and dried in air. Yield: 25.1% based on L. Our attempts to get single crystals of **2** by different methods were in vain. Elem. anal. Calcd (%) for $C_9H_8CoN_2O_6$: C, 36.10; H, 2.70; N, 9.37. Found: C, 36.40; H, 3.00; N, 9.40. IR (cm^{-1}, KBr): 2168 s, 1632 s, 1564 m; 1452w 1383 s, 1327 m, 759 m, 688 m, 673 m.

2.4 Physical measurements

Elemental analyses were determined on an Elementar Vario ELIII analyzer. The FT-IR spectra were recorded in the range 500–4000 cm^{-1} using KBr pellets on a Nicolet NEXUS 670 spectrophotometer. Powder X-ray diffraction data were collected on a Bruker D8-ADVANCE diffractometer equipped with Cu Kα at a scan speed of 1 min^{-1}. Temperature and field dependent magnetic measurements were performed on a Quantum Design MPMS-XL5 SQUID magnetometer. The experimental susceptibilities were corrected for the diamagnetism of the constituent atoms (Pascal's tables).

2.5 X-ray crystallographic measurements

Diffraction data for **1** was collected at 293 K on a Bruker Apex II CCD area detector equipped with graphite-monochromated Mo Kα radiation ($\lambda = 0.71073$ Å). Empirical absorption corrections were applied using the SADABS program.[15] The structures were solved by the direct method and refined by the full-matrix least-squares method on F^2, with all non-hydrogen atoms refined with anisotropic thermal parameters.[16] All the hydrogen atoms attached to carbon atoms were placed in calculated positions and refined using the riding model, and the water hydrogen atoms were located from the difference maps. Selected crystal data are listed in Table 1 and the selected bond lengths and angles in Table 2.

Table 1 Crystal data and structure refinement for **1**

Formula	$C_9H_8MnN_2O_6$
M_r	295.12
Crystal system	Orthorhombic
Space group	*Pnma*
a (Å)	7.621(5)
b (Å)	7.519(5)
c (Å)	18.177(13)
V (Å^3)	1041.7(13)
Z	4
ρ_{calc} (Mg/m^3)	1.882
μ (mm^{-1})	1.291
Refl. collected/unique	4917/1243
R_{int}	0.0991
GOF	1.170
R_1 [$I>2\sigma(I)$]	0.0779
wR_2 (all data)	0.1676

Table 2 Selected bond [Å] and angles [°] for compound **1**

Bond	Distance	Bond	Distance
Mn1–O2B	2.159(5)	Mn1–O1	2.172(4)
Mn1–N2	2.234(4)	O2C–Mn1–O1	88.9(2)
O2B–Mn1–O2C	180.00	O2B–Mn1–O1	91.1(2)
O2B–Mn1–N2	88.5(2)	O2C–Mn1–N2	91.5(2)
O1–Mn1–N2	92.4(2)	O1A–Mn1–N2	87.6(2)
C1–O1–Mn1	135.0(5)	Mn(1)E–N(2)–Mn(1)	114.6(3)
N2–Mn1–N2E	180.00	O1–Mn1–O1A	180.00

Symmetry codes: A: $-x+1, -y, -z+1$; B: $-x+3/2, -y, z-1/2$; C: $x-1/2, y, -z+3/2$; D: $x, -y+1/2, z$; E: $-x+1, y-1/2, -z+1$.

We were unable to determine the single-crystal structure of **2**, but the powder X-ray diffraction pattern of the compound is similar to that of **1**, with some shifts in peak positions, suggesting isomorphism. The unit cell refinement using the CELREF program[17] based on the same orthorhombic space group yielded $a = 7.551(4)$ Å, $b = 7.317(4)$ Å, $c = 18.373(9)$ Å, and $V = 1015.1(9)$ Å^3 (see ESI†). The changes in the unit cell dimensions of **2** with respect to **1** is consistent with the peak shifts in the powder X-ray diffraction pattern, and the contraction of the cell volume of **2** is in agreement with the smaller ionic radius of Co(II) with respect to Mn(II).

3 Results and discussion

3.1 Crystal structure

The structure of **1** was determined by single crystal X-ray analyses. The coordination environment of the Mn(II) ion is shown in Fig. 1, and selected bond distances and angles are given in Table 2. Mn(II) adopts a centrosymmetric *trans*-octahedral geometry with a slight axial elongation. The equatorial plane is defined by four carboxylate oxygens (Mn1–O1, 2.172(4) Å, Mn1–O2, 2.159(5) Å), with two nitrogen atoms from cyanate ions (Mn1–N2, 2.234(4) Å) at the axial sites. Adjacent Mn(II) ions [M $\cdots$ M = 3.76(3) Å] are linked by an N–EO cyanate bridge [M–N–M = 114.6(3)°] and two

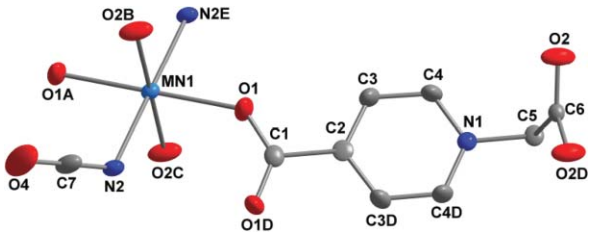

Fig. 1 The local coordination environment of the Mn center in compound **1** with the atom labeling scheme (Hydrogen atoms were omitted for clarity). The thermal ellipsoids were drawn at 30% probability. Symmetry code: A $-x+1, -y, -z+1$, B $-x+3/2, -y, z-1/2$, C $x-1/2, y, -z+3/2$, D $x, -y+1/2, z$, E $-x+1, y-1/2, -z+1$.

syn–syn carboxylate bridges, yielding a uniform chain of corner-shared octahedra (Fig. 2a). Adjacent octahedra in the chain are slanted towards each other with an angle of 59.9° between the equatorial planes. Each chain is linked to four others by L ligands to produce a 3D network. The shortest interchain M···M distance is 7.621(3) Å, and that spanned by L is 9.855(3) Å. The linkers divide the interchain space into small channels, in which water molecules are enclosed.

The 3D network is similar to that for the previous $[VO(BDC)]_n$ compound (BDC = 1,4-benzenedicarboxylate), which contains interlinked chains with mixed $(\mu_2\text{-O})(\mu_2\text{-COO})_2$ bridges.[18] According to Yaghi *et al.*, the carboxylate carbon atoms in the chains can be connected to form zig-zag ladder-shaped secondary building units (SBUs, Fig. 2b), which are interlinked into a 3D **sra** net[18,19] (Schläfli vertex symbol $4^2 \times 6^3 \times 8$) by organic linkers (Fig. 2e). A simpler representation of the evolution of the 3D net is given in Fig. 2c and 2f, which clearly show the alternating connection of the neighboring chains (represented as thick rods) by the organic linkers (thin rods).

3.2 IR specta

The IR spectra of the two compounds are similar. They exhibit strong absorptions at about 1630 and 1384 cm^{-1}, assignable to the asymmetric and symmetric stretching vibrations of the carboxylate groups, respectively. The very strong bands at about 2170 (**1**) and 2168 (**2**) cm^{-1} are due to the ν(NC) absorption of the cyanate ligand.[20] As to the coordination mode of cyanate (N- or O-bonded), it has been claimed that the ν(CN) band cannot give unambiguous information while the ν(CO) frequency may be the best IR criterion.[20] In our compounds, the medium bands at about 1325 are attributable to ν(CO). The frequencies are higher than that for free cyanate and fall in the usual range of 1300–1350 cm^{-1} for N-bonded cyanate (isocyanate).[20] The IR spectra in the 600–640 cm^{-1} range are too complex to assign the δ(NCO) absorptions, which have sometimes been used as diagnostic signals for simple compounds. Further evidences of the N-bonded mode come from the crystallographic refinement parameters. The final refinements with O-bonded cyanate led to increased R_1 and wR_2 parameters and increased residue peaks in the difference map.

3.3 Magnetic properties

Complex 1. The magnetic susceptibility of complex **1** was measured under 1 kOe in the 2–300 K temperature range and is shown as $\chi_M T$ and χ_M *versus* T plots in Fig. 3. The measured $\chi_M T$ value at 300 K is about 3.85 emu mol^{-1} K, lower than the spin-only value (4.38 emu mol^{-1} K) for a high-spin Mn(II) ion. Upon cooling, the $\chi_M T$ value decreases monotonically and tends to zero at low temperature, while the χ_M value increases to a rounded maximum of 5.0×10^{-2} emu mol^{-1} K at *ca.* 24 K and then drops rapidly. These features indicate dominant antiferromagnetic coupling between neighboring manganese(II) ions.

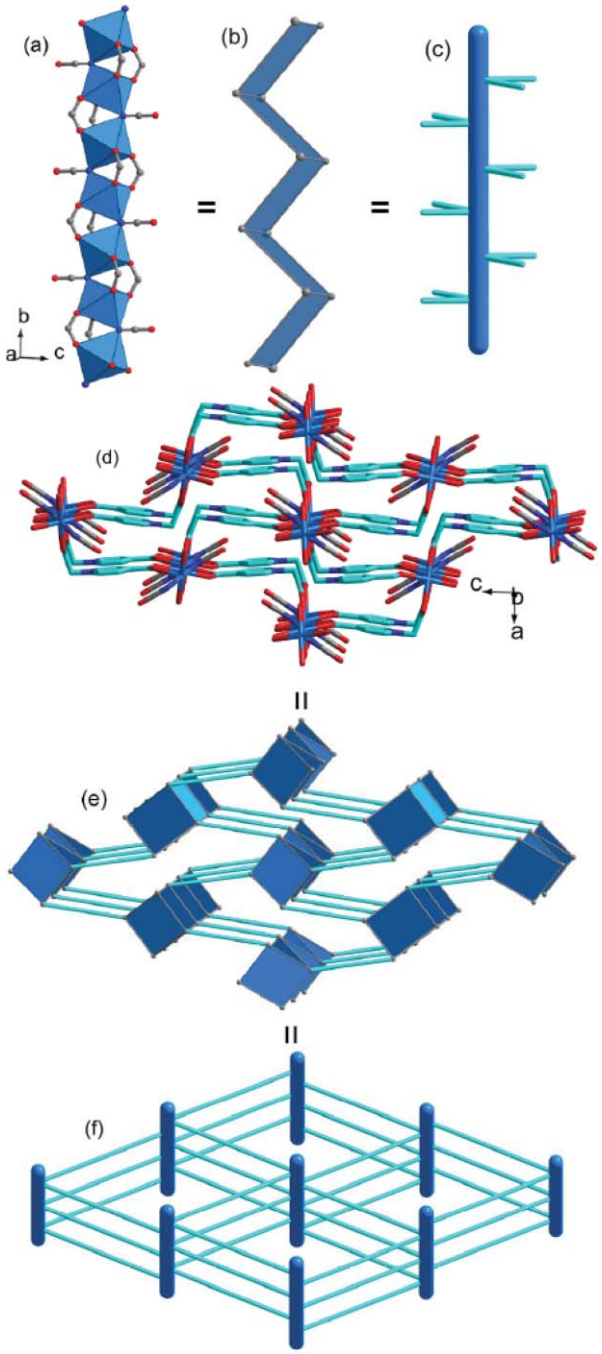

Fig. 2 The structural and topological representations of the 1D chain and the 3D framework of compound **1** (see the text for details).

Despite the 3D structural features, the system can be regarded as isolated 1D chains from the magnetic viewpoint, because the magnetic interactions through the long non-conjugated L ligand should be negligible. Thus, the data of **1** over the whole temperature

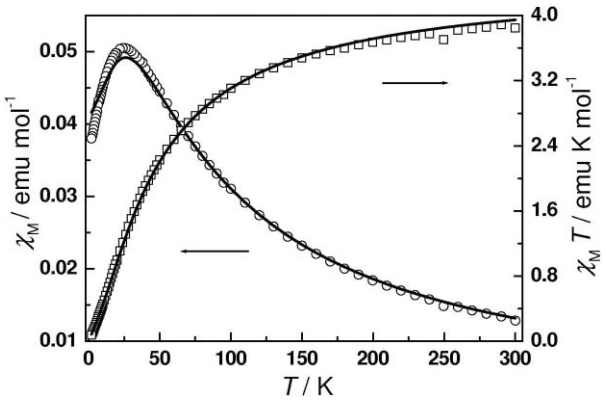

Fig. 3 Temperature dependence of χ and χT for **1**. The solid lines represent the fit to the conversional equation derived by Fisher for a uniform chain (see text).

range were fitted to the well-known expression proposed by Fisher for 1D uniform chains of classical spins[21]:

$$\chi_{chain} = [Ng^2\beta^2S(S + 1)/(3kT)][(1- u)/(1 + u)]$$

where $u = \coth[JS(S + 1)/kT] - kT/[JS(S + 1)]$, J is based on the spin Hamiltonian $\boldsymbol{H} = J\Sigma \boldsymbol{S}_i\boldsymbol{S}_{i+1}$ with $S = 5/2$. The best fit led to $J = -4.3$ cm^{-1} with g fixed at 2.00. The negative value of J confirms the antiferromagnetic nature of the coupling through the mixed triple bridges.

Complex 2. Magnetic measurements were carried out on a polycrystalline sample of **2** at an applied field of 200 Oe (Fig. 4). The χT value per formula at 300 K is *ca.* 3.43 cm^3 mol^{-1} K, much higher than the spin-only value of 1.88 cm^3 mol^{-1} K for $S = 3/2$, indicating the significant orbital contribution typical of high-spin Co(II) in an octahedral surrounding. The χ^{-1} *versus* T plot above 50 K follows the Curie–Weiss law with $C = 3.57$ emu mol^{-1} K and $\theta = -12.0$ K. As the temperature is lowered, while the χ value increases monotonically, χT first decreases slowly to a broad minimum around 45 K, then increases to a maximum of 19.65 cm^3 mol^{-1} K at 2.3 K, and finally drops to 19.11 emu mol^{-1} K at 2 K. Such a complex temperature-dependent behavior of χT is the consequence of the interplay and competition of several concurrent effects, including the single-ion effects (first-order spin-orbital coupling and ligand-field distortion of Co(II) sites) and intrachain magnetic interactions between Co(II) ions. The increase of χT in the low temperature range from 45 to 2.3 K suggests that ferromagnetic coupling between neighboring Co(II) ions are mediated through the 3-fold (μ_2-NCO)(μ_2-COO)$_2$ bridge, while the fall of the χT value from 300 to 45 K and the negative θ value above 50 K suggest that the ferromagnetic effect is overcompensated by the single-ion effects in the high temperature range. The final decrease of χT for compound **2** may be attributed to the saturation effect and/or the presence of interchain antiferromagnetic interactions.

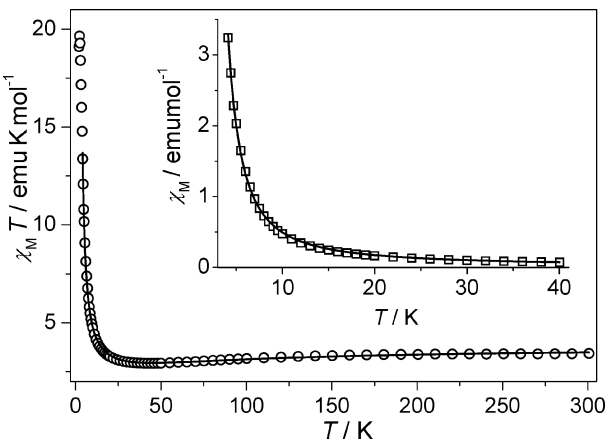

Fig. 4 Temperature dependence of χT for **2**. Inset: amplified temperature dependence of χ *versus* T in the region of low temperature for **2**. The solid line represents the fit to the Ising model.

The ferromagnetic coupling is also supported by the isothermal magnetization measured at 2 K (Fig. 5), which rises very rapidly in the low field region. The magnetization of **2** is 2.64 Nβ at 50 kOe, which is in the usual range of 2–3 Nβ for Co(II).[22] It is noted that the value of **2** tends to increase upon further increasing the field above 50 kOe. This behavior is typical of Co(II) systems with large magnetic anisotropy. Further magnetic measurements revealed no indication of long-range ordering (no hysteresis and no out-of-phase ac susceptibility signals).

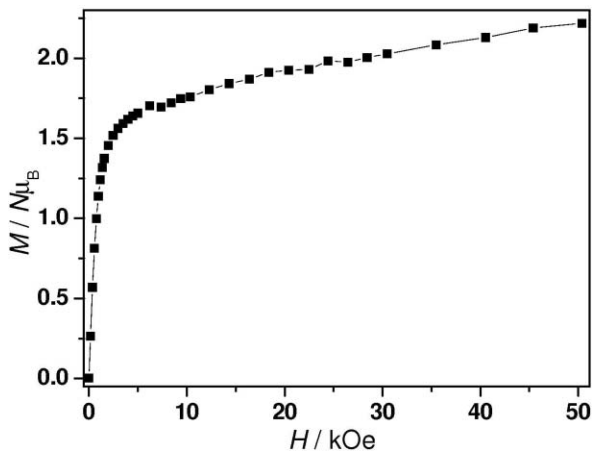

Fig. 5 Magnetization curves at 2 K for compound **2**.

It is well known that octahedral cobalt(II) may be handled as an Ising-like ion with effective $S_{eff} = 1/2$ spin at low temperature, as a result of spin-orbital coupling. Thus the fit of the low-temperature χ data to the Ising chain model[23] was attempted using the following expressions based on the Hamiltonian $\boldsymbol{H} = -J\Sigma \boldsymbol{S}_i\boldsymbol{S}_{i+1}$:

$$\chi = (\chi_{\parallel} + 2\chi_{\perp})/3,$$

$$\text{with } \chi_{\parallel} = (N\beta^2g_{\parallel}{}^2/4kT)\exp(J/2kT)$$

$$\chi_{\perp} = (N\beta^2g_{\perp}{}^2/2J)[\tanh(J/4kT) + (J/2kT)\,\mathrm{sech}^2(J/4kT)]$$

The data between 4 and 40 K are well simulated by the expressions with $J = 9.8$ cm^{-1}, $g_{\parallel} = 8.8$ and $g_{\perp} = 0$ (Fig. 4). The zero value of $g_{\perp}$ confirms the strong Ising-like anisotropy of the system. The relationship that χT ($= \chi_{\parallel} T/3$) $\propto \exp(-J/kT)$ suggests that the $\ln(\chi T)$ value in the range 4–40 K increases linearly with $1/T$. This behavior is characteristic of 1D systems with uniaxial anisotropy.[24]

Alternatively, the high-temperature data were analyzed using the phenomenological approach proposed by Rueff *et al.*[25] for low-dimensional Co(II) systems:

$$\chi_M T = A \exp(-E_1/kT) + B \exp(-E_2/kT)$$

in which $A + B$ equals the Curie constant, and E_1, E_2 represent the "activation energies" corresponding to single-ion effects (the spin-orbit coupling and site distortion) and the magnetic exchange interactions, respectively. This approach allows one to have a rough estimation of the strength of the magnetic exchange interactions. Very good results have been reported in 1D and 2D Co(II) complexes. In almost all of these complexes, E_1/k, spin-orbit coupling and site distortion, is on the order of +100 K. As shown in Fig. 4, the fit using the above expression is quite satisfactory above 4 K. The values obtained are $A + B = 3.78$ cm^3 K mol^{-1}, $E_1/k = +57.2$ K, and $E_2/k = -5.1$ K. The $A + B$ value is comparable with the Curie constant obtained by the Cure–Weiss fitting (see above) and agreeable with the constant reported in the literature. The E_1/k value accounting for the effect of spin-orbit coupling and site distortion is also consistent with literature values (of the order of +100 K). The sign of $-E_2/k$ clearly indicates ferromagnetic exchange interactions. The value corresponds to $J/k = 10.2$ K (*i.e.*, $J = 7.1$ cm^{-1}) according to the Ising chain approximation, $\chi_M T \propto \exp(J/2kT)$. It is interesting to note that this J value is comparable with the $J = 9.8$ cm^{-1} value obtained from the Ising model fitting in the 4–40 K range.

The magnetic analyses on compounds **1** and **2** raise an interesting issue concerning the nature of magnetic interactions for different metal ions in isomorphous structures. The observation in these compounds with $(\mu_2\text{-NCO})(\mu_2\text{-COO})_2$ triple bridges is similar to that for a series of compounds with $(\mu_2\text{-N}_3)_2(\mu_2\text{-COO})$ triple bridges, which mediate antiferromagnetic coupling in Mn(II) species but ferromagnetic coupling in Co(II) and Ni(II) species.[13c] As has been discussed for these previous systems[13c] and the metal dicyanamide series of $M[N(CN)_2]_2$,[26,27] the magnetic change may be related to the different $t_{2g}^{x}e_g^{y}$ configurations for the octahedral metal centers. It was proposed that the t_{2g}–e_g superexchange between the metal ions is antiferromagnetic while the t_{2g}–t_{2g} and e_g–e_g combinations are ferromagnetic. The relative number and magnitude of these exchange contributions determine the nature of the overall coupling. From Ni(II) systems ($t_{2g}^6e_g^2$), only e_g–e_g combinations operate to give ferromagnetic coupling. For Co(II) ($t_{2g}^5e_g^2$), the t_{2g}–e_g antiferromagnetic contributions are not strong enough to compensate the t_{2g}–t_{2g} and e_g–e_g ferromagnetic exchange. For Mn(II) ($t_{2g}^3e_g^2$), however, the t_{2g}–e_g antiferromagnetic contributions increase greatly in number and overtake the ferromagnetic exchange, leading to net antiferromagnetic interactions.

It is also worthwhile comparing the magnetic properties of the azide and cyanate systems with similar bridging networks. Only a Mn(II) species with the $(\mu_2\text{-N}_3)(\mu_2\text{-COO})_2$ triple bridges, which also contains uniform chains, is available in the literature.[13b] With similar Mn$\cdots$Mn distances and Mn–N–Mn angles, it is noted that the substitution of azide by cyanate in the triple bridge leads to an increase in magnetic coupling ($J = -4.3$ cm^{-1} for **1** *versus* -3.0 cm^{-1} for the azide analogue). Generally, the overall magnetic coupling through coexistent bridges is the concurrent effect of the individual pathways. It has been established that the *syn–syn* carboxylate bridge is an universal antiferromagnetic pathway because it induces a good overlap of magnetic orbitals.[11,28] For the EO azide bridge, density function theory (DFT) calculations[29] on Mn(II) systems suggest that the exchange is ferromagnetic for $\theta > 98°$, as experimentally observed in a number of species with $\theta = 100$–$105°$.[3a,5c] In our previous compound, $\theta = 111°$,[13b] ferromagnetic exchange could thus be expected through the azide pathway. The observed antiferromagnetic interaction suggests that the antiferromagnetic pathway through carboxylate dominates to give a negative J value. We have not found any magnetic studies on EO–cyanate-bridged Mn(II) systems, but theoretical and experimental studies on a few Ni(II) systems have suggested that the EO–cyanate bridge transmits much weaker ferromagnetic interactions than EO–azide.[6] It is most likely that the EO–cyanate bridge in **1** also transmits ferromagnetic exchange, but this ferromagnetic pathway is less efficient than azide, so the overall antiferromagnetic coupling in the cyanate–carboxylate system is stronger than that in the azide–carboxylate system.

The EO–cyanate bridge has been reported to be responsible for the ferromagnetic coupling in Co(II) clusters with mixed cyanate and oxo bridges.[7c,d] The results for **2** suggest that the ferromagnetic cyanate pathway dominates over the antiferromagnetic carboxylate pathways. No Co(II) systems with $(\mu_2\text{-N}_3)(\mu_2\text{-COO})_2$ triple bridges are available for comparison. We can anticipate an increased ferromagnetic interaction if the cyanate bridge in **2** is replaced by azide, which is a more efficient ferromagnetic mediator. This assumption is yet to be confirmed by experimental results.

4 Conclusion

We have described the structure and magnetic properties of Mn(II) and Co(II) compounds with mixed cyanate and inner-salt dicarboxylate ligands. In the isomorphic compounds, the anionic uniform chains with mixed triple bridges (one EO cyanate and two *syn–syn* carboxylate) are cross-linked by the cationic 1-methylpyridinium spacers to give a 3D structure. They are the first systems with mixed cyanate and carboxylate bridges. It has been demonstrated that the magnetic coupling through the triple bridges is antiferromagnetic in the Mn(II) compound but ferromagnetic in the Co(II) species.

Acknowledgements

We are thankful for the financial support from NSFC (20771038) and Shanghai Leading Academic Discipline Project (B409).

Notes and references

1 J. S. Miller, M. E. Drilon, *Magnetism: Molecules to Materials* Wiley-VCH: Weinheim, 2002-2005; Vol. I-V.
2 (*a*) O. Kahn, *Molecular Magnetism*VCH: New York, 1993; (*b*) J. S. Miller and A. J. Epstein, *Angew. Chem.*, 1994, **106**, 399; J. S. Miller and A. J. Epstein, *Angew. Chem., Int. Ed. Engl.*, 1994, **33**, 385; (*c*) *Molecular Magnetism: from Molecular Assemblies to Devices*, ed. E. Coronado, P. Delhaes, D. Gatteschi, and J. S. Miller, NATO ASI Series, Kluwer, Dordrecht, 1995, vol. **321**.
3 (*a*) J. Ribasa, A. Escuer, M. Monfort, R. Vicente, R. Cortés, L. Lezama and T. Rojo, *Coord. Chem. Rev.*, 1999, **193–195**, 1027; (*b*) Y.-F. Zeng, X. Hu, F.-C. Liu and X.-H. Bu, *Chem. Soc. Rev.*, 2009, **38**, 469; (*c*) X.-Y. Wang, Z.-M. Wang and S. Gao, *Chem. Commun.*, 2008, (3), 281.
4 (*a*) E.-Q. Gao, Y.-F. Yue, S.-Q. Bai, Z. He and C.-H. Yan, *J. Am. Chem. Soc.*, 2004, **126**, 1419; (*b*) E.-Q. Gao, S.-Q. Bai, Z.-M. Wang and C.-H. Yan, *J. Am. Chem. Soc.*, 2003, **125**, 4984; (*c*) E.-Q. Gao, P.-P. Liu, Y.-Q.

Wang, Q. Yue and Q.-L. Wang, *Chem.–Eur. J.*, 2009, **15**, 1217; (*d*) P.-P. Liu, A.-L. Cheng, N. Liu, W.-W. Sun and E.-Q. Gao, *Chem. Mater.*, 2007, 2726.
5 (*a*) T. C. Stamatatos, K. A. Abboud, W. Wernsdorfer and G. Christou, *Angew. Chem., Int. Ed.*, 2007, **46**, 884; (*b*) C. I. Yang, W. Wernsdorfer, G. H. Lee and H. L. Tsai, *J. Am. Chem. Soc.*, 2007, **129**, 456; (*c*) M.-M. Yu, Z.-H. Ni, C.-C. Zhao, A.-L. Cui and H.-Z. Kou, *Eur. J. Inorg. Chem.*, 2007, (36), 5670; (*d*) A. Escuer, F. A. Mautner, M. A. S. Goher, M. A. M. Abu-Youssef and R. Vicente, *Chem. Commun.*, 2005, (5), 605; (*e*) A. Escuer and G. Aromí, *Eur. J. Inorg. Chem.*, 2006, (23), 4721.
6 (*a*) M. Habib, T. K. Karmakar, G. Aromí, J. Ribas-Ariño, H. K. Fun, S. Chantrapromma and S. K. Chandra, *Inorg. Chem.*, 2008, **47**, 4109; (*b*) M. I. Arriortua, R. Cortés, J. L. Mesa, L. Lezama, T. Rojo and G. Villeneuve, *Transition Met. Chem.*, 1988, **13**, 371.
7 (*a*) C. Diaz, J. Ribas, M. S. El Fallah, X. Solans and M. Font-Bardí, *Inorg. Chim. Acta*, 2001, **312**, 1; (*b*) M. A. S. Goher and F. A. Mautner, *J. Chem. Soc., Dalton Trans.*, 1999, (12), 1923; (*c*) M. G. Barandika, Z. Serna, R. Cortés, L. Lezama, M. K. Urtiaga, M. I. Arriortuac and T. Rojo, *Chem. Commun.*, 2001, 45; (*d*) Z. E. Serna, M. K. Urtiaga, M. G. Barandika, R. Cortés, S. Martin, L. Lezama, M. I. Arriortua and T. Rojo, *Inorg. Chem.*, 2001, **40**, 4550; (*e*) P. Talukder, A. Datta, S. Mitra, G. Rosair, M. S. El Fallah and J. Ribas, *Dalton Trans.*, 2004, 4161; (*f*) M. G. B. Drew, C. J. Harding and J. Nelson, *Inorg. Chim. Acta*, 1996, **246**(1–2), 73.
8 (*a*) S. Youngme, J. Phatchimkun, U. Suksangpanya, C. Pakawatchai, G. A. van Albada and J. Reedijk, *Inorg. Chem. Commun.*, 2005, **8**, 882; (*b*) T. Mallah, M.-L. Boillot, O. Kahn, J. Gouteron, S. Jeannin and Y. Jeannin, *Inorg. Chem.*, 1986, **25**, 3058; (*c*) T. Mallah, O. Kahn, J. Gouteron, S. Jeannin, Y. Jeannin and C. J. O'Connor, *Inorg. Chem.*, 1987, **26**, 1375; (*d*) M. S. El Fallah, A. Escuer, R. Vicente, F. Badyine, X. Solans and M. Font-Bardia, *Inorg. Chem.*, 2004, **43**, 7218; (*e*) T. Otieno, S. J. Rettig, R. C. Thompson and J. Trotter, *Inorg. Chem.*, 1993, **32**, 4384; (*f*) A. Escuer, M. Font-Bardía, E. Peñalba, X. Solans and R. Vicente, *Inorg. Chim. Acta*, 1999, **286**, 189; (*g*) H. Grove, M. Julve, F. Lloret, P. E. Kruger, K. W. Törnroos and J. Sletten, *Inorg. Chim. Acta*, 2001, **325**(1–2), 115; (*h*) Z.-N. Chen, H.-X. Zhang, K.-B. Yu, K.-C. Zheng, H. Cai and B.-S. Kang, *J. Chem. Soc., Dalton Trans.*, 1998, (7), 1133.
9 (*a*) S. Deoghoria, S. Sain, B. Moulton, M. J. Zaworotko, S. K. Bera and S. K. Chandra, *Polyhedron*, 2002, **21**, 2457; (*b*) S. K. Dey, N. Mondal, M. S. El Fallah, R. Vicente, A. Escuer, X. Solans, M. Font-Bardía, T. Matsushita, V. Gramlich and S. Mitra, *Inorg. Chem.*, 2004, **43**, 2427.
10 (*a*) T. Liu, Y.-J. Zhang, Z.-M. Wang and S. Gao, *Inorg. Chem.*, 2006, **45**, 2782; (*b*) C. J. Milios, A. Prescimone, J. Sanchez-Benitez, S. Parsons, M. Murrie and E. K. Brechin, *Inorg. Chem.*, 2006, **45**, 7053.
11 (*a*) Z. He, Z.-M. Wang, S. Gao and C.-H. Yan, *Inorg. Chem.*, 2006, **45**(17), 6694.
12 (*a*) F.-C. Liu, Y.-F. Zeng, J. Jiao, X.-H. Bu, J. Ribas and S. R. Batten, *Inorg. Chem.*, 2006, **45**, 2776; (*b*) Y.-F. Zeng, J.-P. Zhao, B.-W. Hu, X. Hu, F.-C. Liu, J. Ribas, J. R. Arino and X.-H. Bu, *Chem.–Eur. J.*, 2007, **13**(35), 9924; (*c*) F.-C. Liu, Y.-F. Zeng, J.-R. Li, X.-H. Bu, H.-J. Zhang and J. Ribas, *Inorg. Chem.*, 2005, **44**(21), 7298.
13 (*a*) Y.-Q. Wang, J.-Y. Zhang, Q.-X. Jia, E.-Q. Gao and C.-M. Liu, *Inorg. Chem.*, 2009, **48**, 789; (*b*) C.-Y. Tian, W.-W. Sun, Q.-X. Jia, H. Tian, and E.-Q. Gao, DOI: 10.1039/b900110g; (*c*) Y. Ma, J.-Y. Zhang, A.-L. Cheng, Q. Sun, E.-Q. Gao and C.-M. Liu, *Inorg. Chem.*, 2009, **48**(13), 6142.
14 X.-B. Wang, J. E. Dacres, X. Yang, K.-M. Broadus, L. Lis, L.-S. Wang and S.-R. Kass, *J. Am. Chem. Soc.*, 2003, **125**, 296.
15 G. M. Sheldrick, *Program for Empirical Absorption Correction of Area Detector Data*University of Göttingen, Germany, 1996.
16 (*a*) G. M. Sheldrick, *SHELXTL Version 5.1*. Bruker Analytical X-ray Instruments Inc., Madison, Wisconsin, USA, 1998; (*b*) G. M. Sheldrick, *SHELXL-97, PC Version*. University of Göttingen, Germany, 1997.
17 J. Laugier, and B. Bochu, *LMGP, Suite of Programs for the interpretation of X-ray Experiments*, ENSP/Laboratoire des Matériaux et de Génie Physique, Saint Martin d'Hères, France, http://www.inpg.fr/LMGP.
18 N. L. Rosi, J. Kim, M. Eddaoudi, B.-L. Chen, M. O'Keeffe and O. M. Yaghi, *J. Am. Chem. Soc.*, 2005, **127**, 1504.
19 M. O'Keeffe, M. A. Peskov, S. J. Ramsden and O. M. Yaghi, *Acc. Chem. Res.*, 2008, **41**(12), 1782. See also: Reticular Chemistry Structure Resource (RCSR), http://rcsr.anu.edu.au/. The three-letter sra symbol comes from $SrAl_2$, and the net corresponds to the Al framework in $SrAl_2$.
20 J. Martínez-Lillo, D. Armentano, G.-D. Munno, F. Lloret, M. Julve and J. Faus, *Inorg. Chim. Acta*, 2006, **359**(13), 4343.
21 M. E. Fisher, *Am. J. Phys.*, 1964, **32**, 343.
22 H.-S. Yoo, J. II. Kim, N. Yang, E.-K. Koh, J.-G. Park and C. S. Hong, *Inorg. Chem.*, 2007, **46**, 9054.
23 M. Sato, H. Kon, H. Akoh, A. Tasaki, C. Kabuto and J.-V. Silverton, *Chem. Phys.*, 1976, **16**, 405.
24 C. Coulon, H. Miyasaka and R. Clérac, *Struct. Bonding*, 2006, **122**, 163.
25 (*a*) J.-M. Rueff, N. Masciocchi, P. Rabu, A. Sironi and A. Skoulios, *Chem.–Eur. J.*, 2002, **8**(8), 1813; (*b*) J.-M. Rueff, N. Masciocchi, P. Rabu, A. Sironi and A. Skoulios, *Eur. J. Inorg. Chem.*, 2001, (11), 2843.
26 S. R. Batten, P. Jensen, C. J. Kepert, M. Kurmoo, B. Moubaraki, K. S. Murray and D. J. Price, *J. Chem. Soc., Dalton Trans.*, 1999, (17), 2987.
27 C. R. Kmety, Q. Huang, J. W. Lynn, R. W. Erwin, J. L. Manson, S. McCall, J. E. Crow, K. L. Stevenson, J. S. Miller and A. J. Epstein, *Phys. Rev.*, 2000, **B62**, 5576.
28 T. Cauchy, E. Ruiz and S. Alvarez, *J. Am. Chem. Soc.*, 2006, **128**, 15722.
29 E. Ruiz, J. Cano, S. Alvarez and P. Alemany, *J. Am. Chem. Soc.*, 1998, **120**(43), 11122.